

# Kinetics of Modulated and Ordered Structures in CuAu.

K. R. Elder<sup>1,4</sup>, Nicholas A. Gross<sup>2,3</sup>, Bulbul Chakraborty<sup>3</sup> and Nigel Goldenfeld<sup>4</sup>.

<sup>1</sup> *Department of Physics, Oakland University, Rochester, MI, 48309-4401*

<sup>2</sup> *Boston University, College of General Studies, 981 Commonwealth Ave., Boston, MA 02215.*

<sup>3</sup> *Physics Department, Brandeis University, Waltham, MA 02254.*

<sup>4</sup> *Department of Physics, University of Illinois at Urbana-Champaign, 1110 West Green Street, Urbana, Illinois 61801.*  
(August 15, 2018)

A continuum model derived from an atomistic Hamiltonian is used to examine the ordering kinetics in CuAu. A detailed description of the formation of the low and high temperature ordered and modulated superlattice states is given. The metastability of the modulated phase at low temperatures is shown to severely hinder creation of the ordered superlattice. Formation of the modulated superlattice is shown to result in interesting lamellar and labyrinthine structures.

05.70.Ln,64.60.Cn,81.30.Hd

The vast majority of synthetic and naturally occurring materials contain long-lived non-equilibrium morphologies which determine material properties. Understanding the non-equilibrium or kinetic processes that lead to such microscopic structures is, therefore, one of the most important tasks facing materials theory. The binary alloy CuAu is an excellent material to study such processes for the following reasons: the existence of a modulated superlattice at intermediate temperatures gives rise to a rich set of phase transformations and microstructures; the kinetics are accessible in x-ray scattering experiments; and a continuum model for the kinetics has been derived from a quantum mechanical description of this alloy [1]. In this paper the continuum model will be used to provide a detailed theoretical description of the non-equilibrium processes that occur in CuAu. Thus predictions that can be verified experimentally are obtained from a microscopic description of the alloy.

The continuum model predicts two first order phase transitions; one from a disordered superlattice to a modulated superlattice at  $T = T_{MD}$  and the other from the modulated phase to an ordered superlattice at  $T = T_{OM}$  (where  $T_{OM} < T_{MD}$ ). The purpose of this paper is to determine the transient morphologies that arise following instantaneous temperature quenches that bring the system from one equilibrium state to another. The results of this study indicate that: the ordered superlattice is difficult to form just below  $T_{OM}$  due to the creation of a long-lived metastable modulated phase; the growth of an ordered phase far below  $T_{OM}$  is hindered by the presence of ‘terminal’ droplets; and the nucleation of the modulated phase from the low and high temperature phases leads to labyrinthine and lamellar patterns respectively.

The appearance of the modulated superlattice was predicted from an atomistic model by Chakraborty and Xi

[1]. In this work, effective medium theory [2,3] was employed to obtain an approximate classical Hamiltonian from a full quantum mechanical model. A mean field analysis of this Hamiltonian was used to obtain the free energy as a function of the average sublattice concentration ( $\eta$ ) along one degenerate ordering direction. This degeneracy can lead to interesting effects but will not be considered here. The free energy can be written,

$$\mathcal{F}(\eta) = \mathcal{F}_o + (2\pi/a)^d \int d\vec{r} [a_T \eta^2 - u \eta^4 + v \eta^6 - e |\vec{\nabla}_\perp \eta|^2 + e |\vec{\nabla}_\parallel \eta|^2 + f (\nabla_\perp^2 \eta)^2], \quad (1)$$

where,  $a_T = 0.042 \Delta T \text{ meV/K}$ ,  $\Delta T = T - T_o$ ,  $T_o = 1219 \text{ K}$ ,  $u = 5.25 \text{ meV}$ ,  $v = 6.1 \text{ meV}$ ,  $e = 25.5 \text{ meV}/(2\pi/a)^2$  and  $f = 195.5 \text{ meV}/(2\pi/a)^4$  and  $a$  is the shortest lattice parameter in the tetragonal structure of the low temperature CuAu(I) ordered phase. The symbols  $\nabla_\perp$  and  $\nabla_\parallel$  refer to gradients in the plane perpendicular and parallel to the ordering direction respectively. At low, intermediate and high temperatures  $\mathcal{F}$  is minimized by ordered (i.e.,  $\eta(\vec{x}) = \eta_o \neq 0$ ), modulated (e.g.,  $\eta(x, y, z) = \eta(x + \lambda, y, z)$ ) and disordered (i.e.,  $\eta(\vec{x}) = 0$ ) states respectively. The transitions from the ordered to modulated phase and from the modulated to disordered phase are both first order and respectively occur at  $\Delta T_{OM} \approx -8.0 \text{ K}$ , and  $\Delta T_{MD} \approx 44.4 \text{ K}$  [1,4]. The spinodal temperatures  $T_O^S$  and  $T_M^S$  are defined as the temperatures above which the ordered and modulated phases are unstable, while  $T_D^S$  is defined as the temperature below which the disordered state is unstable to the modulated phase. The values of these temperatures are  $T_O^S = T_o + 35.7 \text{ K}$ ,  $T_M^S = T_o + 52.6 \text{ K}$  and  $T_D^S = T_o + 20.0 \text{ K}$ .

The kinetics are assumed to be relaxational and driven by minimization of the free energy:

$$\partial \eta / \partial t = -\Gamma \delta \mathcal{F} / \delta \eta + \zeta, \quad (2)$$

where  $\zeta$  is a random Gaussian noise term with correlations,  $\langle \zeta(\vec{r}, t) \zeta(\vec{r}', t') \rangle = 2k_B T \Gamma \delta(\vec{r} - \vec{r}') \delta(\tau - \tau')$  and  $k_B$  is the Boltzmann constant. It is convenient to introduce the scaled variables;  $\vec{x} = \vec{r}/\lambda_o$  and  $\tau = t/t_o$  where  $\lambda_o = \sqrt{2f/e}$  and  $t_o = (a/2\pi)^d 2f/(e^2 \Gamma)$  to obtain;

$$\partial \eta / \partial \tau = -(\gamma \Delta T + 2\nabla_\perp^2 + \nabla_\parallel^2 - 2\nabla_\parallel^2) \eta + u' \eta^3 - v' \eta^5 + \nu. \quad (3)$$

Here,  $\gamma = 4a_T f/e^2$ ,  $u' = 8fu/e^2$ ,  $v' = 12fv/e^2$ ,  $\langle \nu(\vec{x}, \tau) \nu(\vec{x}', \tau') \rangle = 2\epsilon \delta(\vec{x} - \vec{x}') \delta(\tau - \tau')$  and  $\epsilon =$

$2k_B T [a/2\pi]^d [2f/e^2] [e/2f]^{d/2}$ . In these rescaled units the modulated wavelength is simply  $2\pi$ . To simplify calculations ordering in the parallel direction will be neglected.

The kinetics that follow a rapid quench are influenced by the modulated phase, even when the pre- and post-quench temperatures are not within the modulated regime. For example, consider the instantaneous quench of a disordered state ( $T_{initial} > T_{MD}$ ) into the ordered regime ( $T_{final} < T_{OM}$ ). The initial response will be to form a modulated type structure, since linear stability analysis predicts that the mode with  $q = 1$  has the largest growth rate [5]. For  $T_{final} < T_{OM}$  the growth of the  $q = 1$  mode is much more rapid than  $q = 0$ , thus a ‘modulated’ structure is quickly formed. Further growth of the  $q = 0$  mode (i.e., the ordered phase) is inhibited by the metastability of the modulated phase. Thus for quenches just below  $T_{OM}$  a long-lived transient modulated phase should develop.

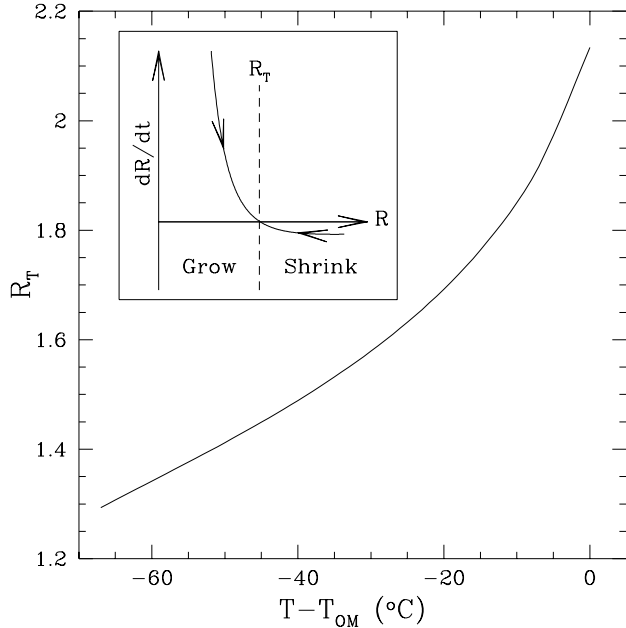


FIG. 1. In this figure the terminal droplet size is shown as a function of temperature. The inset depicts the velocity of the droplet radius as a function of  $R$  as described by Eq. (4).

For  $T_{final} \ll T_{OM}$  the difference between the  $q = 1$  and  $q = 0$  linear growth rates is insufficient to create a modulated structure. The subsequent dynamics do not however reduce to that observed in standard order/disorder transitions in which the average ordered domain size grows as  $t^{1/2}$  [6,7] and droplets shrink at a rate proportional to the curvature. Here a droplet refers to a spherical (or circular in 2-d) regime of one phase (e.g.,  $\eta = -\eta_o$ ) embedded in the other (e.g.,  $\eta = +\eta_o$ ). In CuAu, large droplets shrink but do not disappear. This effect can be traced to the fourth order spatial derivative in the dynamics or equivalently, to the existence of the length scale describing the modulated phase, and to the

two dimensional nature of the ordering process.

To illustrate this effect, consider the dynamics of a single droplet of radius  $R$  in the limit  $R \gg W$ , where  $W$  is the domain wall thickness and is of the order 1. In this limit  $\eta$  can be written  $\eta(r - R(\tau)) \approx \eta^{1d}(r - R(\tau))$ , where  $\eta^{1d}(x)$  is the one-dimensional solution of  $\delta\mathcal{F}/\delta\eta = 0$  with boundary conditions  $\eta(x = \pm\infty) = \pm\eta_o$ . Substituting this result into Eq. (3), multiplying by  $(\partial\eta^{1d}/\partial r)$  and integrating from  $r = 0$  to  $r = \infty$  gives,

$$\partial R/\partial\tau = 2(1 + \sigma_3/\sigma_1)R + 1/R^3, \quad (4)$$

where  $\sigma_i \equiv \int_0^\infty dr (\partial\eta^{1d}/\partial r) (\partial^i \eta^{1d}/\partial r^i)$ . The quantity  $2(1 + \sigma_3/\sigma_1)$  is less than zero for  $T < T_{OM}$ . Thus the droplet will shrink for  $R > R_T$  and grow for  $R < R_T$ , where  $R_T$  is the ‘terminal’ droplet size and is equal to  $R_T = 1/\sqrt{-2(1 + \sigma_3/\sigma_1)}$ . The growth rate of  $R$  is illustrated in the inset of Fig. (1). While this calculation correctly identifies the existence of a terminal droplet, the accuracy is hindered by the approximation  $R \gg W$ . To overcome this obstacle  $R_T$  was determined numerically and the results are shown in Fig. (1).

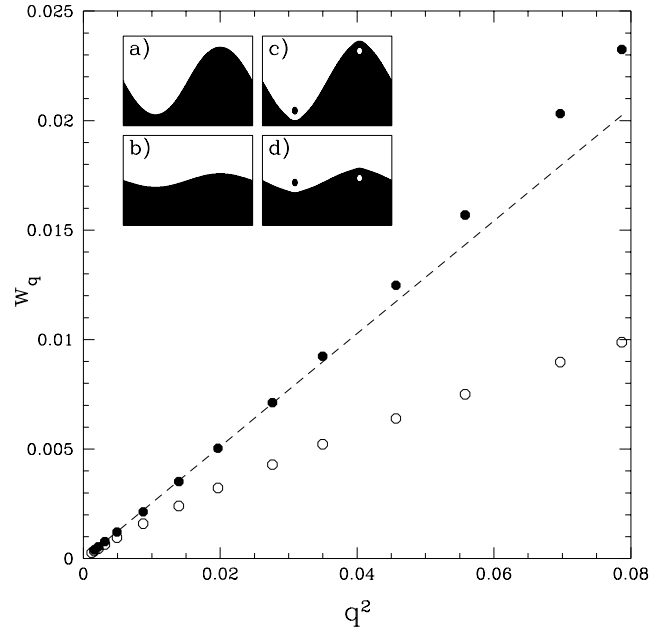


FIG. 2. In this figure the linear dispersion for the position of an antiphase domain boundary is shown as a function of wavevector. The solid and open points represent  $w_q$  in the absence and presence of droplets respectively and the dashed line corresponds to  $w_q \sim q^2$ . In the inset figures (a) and (b) show the interface relaxation in the absence of droplets and in (c) and (d) in the presence of droplets at the same times.

The terminal droplets influence the late stage dynamics by interfering with the motion of antiphase domain walls or interfaces. For comparison it is useful to first consider the interface motion in the absence of droplets. Consider a slowly varying interface such that  $\eta(x, y, \tau) \approx \eta_o$  for  $x > h(y, \tau)$  and  $\eta(x, y, \tau) \approx -\eta_o$  for  $x < h(y, \tau)$ ,

thus defining the position of the antiphase domain wall as  $h(y, t)$ . If  $h(y, t)$  varies slowly in space it is simple to show [4] that  $\partial h/\partial \tau = [-2(1 + \sigma_3/\sigma_1)\nabla^2 + \nabla^4]h$  using the methods discussed in the previous paragraph. The solution in Fourier space is then;  $\hat{h}(q, \tau) = e^{-w_q \tau} \hat{h}(q, 0)$ , where  $w_q = -2(1 + \sigma_3/\sigma_1)q^2 + q^4$ . In the long wavelength limit ( $q \ll 1$ ) this reduces to the standard result for order/disorder transitions (i.e.,  $w_q \sim q^2$ ). To determine the dispersion relationship (i.e.,  $w_q$ ) in the presence of terminal droplets numerical simulations were conducted for the configurations shown in the inset of Fig. (2). The results of these calculations (see Fig. (2)) indicate that the relaxation of the antiphase domain walls is restrained by the terminal droplets. This simple effect will strongly alter the late stage dynamics as the droplets tend to accumulate at interfaces [4]. This accumulation is not due to an attraction between drops and interfaces, but rather by droplets getting swept up by a relaxing interface.

The transient morphologies that emerge in the modulated regime depend on both the pre- and post-quench states. If the pre-quench temperature is above  $T_{MD}$  and the post-quench temperature is between  $T_{OM}$  and  $T_D^S$ ,  $\eta$  is linearly unstable and a convoluted modulated structure will quickly emerge. Similar behavior will be observed if the pre-quench temperature is below  $T_{OM}$  and the post-quench temperature is between  $T_O^S$  and  $T_{MD}$ . In contrast, the kinetics are dominated by nucleation and growth when the pre-quench state is metastable at the post-quench temperature. In addition growth of the nucleated droplets is not a simple process since there is an internal structure within the drops. Each drop will contain a lamellar structure that defines the modulated phase. In general the velocity of the droplet fronts will depend on the orientation of lamella with respect to the droplet front and on the background matrix the droplet is growing in. To understand this effect it is useful to estimate the growth velocities in directions perpendicular and parallel to the lamella as the drop grows into either disordered or ordered backgrounds.

First consider the invasion of the modulated phase into the ordered or disordered phase in a direction parallel to the lamella. The velocity of this front will be denoted  $v_{\parallel}^O$  and  $v_{\parallel}^D$  for propagation into the ordered and disordered phases respectively. To estimate  $v_{\parallel}^D$ ,  $\eta$  can be approximated as  $[\eta_o + \eta^{1d}(y)]F_{\parallel}^O(x, \tau) - \eta_o$ , where  $\eta_o$  is the value of  $\eta$  in the ordered phase,  $\eta^{1d}(y)$  is the one dimensional modulated solution (i.e.,  $\eta^{1d}(y) \approx A \sin(q_o y)$ ) and the overlap function  $F_{\parallel}^D(x, \tau)$  takes the values 1 and 0 in the modulated and ordered phases respectively. Substituting this approximation into Eq. (3), multiplying by  $\eta^{1d}(y)$ , and averaging over one wavelength in  $y$  gives,

$$\begin{aligned} \partial F_{\parallel}^O/\partial \tau = & (1 - \gamma \Delta T + 3\eta_o^3 u' - 5\eta_o^4 v' - \partial_{xxxx})F_{\parallel}^O \\ & + 2\eta_o^2(10v'\eta_o^2 - 3u')(F_{\parallel}^O)^2 \\ & + 3(\eta_o^2 + A^2/4)(u' - 10\eta_o^2 v')(F_{\parallel}^O)^3 \end{aligned}$$

$$\begin{aligned} & + 5v'\eta_o^2(4\eta_o^2 + 3u'A^2)(F_{\parallel}^O)^4 \\ & - 5v'(\eta_o^4 + 3\eta_o A^2/2 + A^4/8)(F_{\parallel}^O)^5. \end{aligned} \quad (5)$$

if  $\eta^{1d}$  is approximated by a single Fourier mode. The front velocity can be obtained by expanding around the zero velocity limit which occurs at  $T = T_{OM}$ . Substituting the approximation,  $F_{\parallel}^O(x, t) \approx f_{\parallel}^O(x - v_{\parallel}^O t)$  (were  $f_{\parallel}^O$  is the solution of Eq. (5) at  $T = T_{OM}$ , with boundary conditions  $f_{\parallel}^O(-\infty) = 1$  and  $f_{\parallel}^O(\infty) = 0$ ) into Eq. (5) and integrating over  $\partial f_{\parallel}^O(x)/\partial x$  gives,

$$v_{\parallel}^O = 0.045(T - T_{OM})/\sigma_{\parallel}^O, \quad (6)$$

where  $\sigma_{\parallel}^O \equiv \int dx (\partial f_{\parallel}^O(x)/\partial x)^2$ . The same techniques can be used to estimate  $v_{\parallel}^D$  and leads to  $v_{\parallel}^D = 0.025(T_{MD} - T)/\sigma_{\parallel}^D$ , where  $\sigma_{\parallel}^D \equiv \int dx (\partial f_{\parallel}^D(x)/\partial x)^2$ , and  $f_{\parallel}^D(x)$  is the solution of Eq. (5) with  $\eta_o = 0$  at  $T = T_{MD}$  and boundary conditions  $f_{\parallel}^D(-\infty) = 1$  and  $f_{\parallel}^D(\infty) = 0$ . Numerically determining  $\sigma_{\parallel}^O$  and  $\sigma_{\parallel}^D$  gives,  $v_{\parallel}^O \approx 0.13(T - T_{OM})$  and  $v_{\parallel}^D \approx 0.12(T_{MD} - T)$ .

Next consider growth in the direction perpendicular to the lamella. For these calculations the velocities will be denoted  $v_{\perp}^O$  and  $v_{\perp}^D$  for growth into the ordered and disordered regimes respectively. To estimate  $v_{\perp}^D$ ,  $\eta$  can be approximated as;  $\eta(x, \tau) \approx \eta^{1d}(x)F_{\perp}^D(x, \tau)$ . Substituting this expression into Eq. (3), multiplying by  $\eta^{1d}(x)$ , averaging over one wavelength and assuming that  $F_{\perp}^D(x, \tau)$  varies slowly in space relative to the modulated wavelength gives,

$$\begin{aligned} \partial F_{\perp}^D/\partial \tau = & (1 - \gamma \Delta T + 4\partial_{xx} - \partial_{xxxx})F_{\perp}^D \\ & + (3u'A^2/4)(F_{\perp}^D)^3 - (5v'A^4/8)(F_{\perp}^D)^5 \end{aligned} \quad (7)$$

if a one mode approximation for  $\eta^{1d}$  is used. Employing the method outlined above gives,  $v_{\perp}^D = 0.025(T_{MD} - T)/\sigma_{\perp}^D$ . Determining  $\sigma_{\perp}^D$  numerically gives  $v_{\perp}^D \approx 0.19(T_{MD} - T)$ . It is much more difficult to estimate  $v_{\perp}^O$  since the solution can not be written as an overlap function times the modulated solution. Numerical attempts to determine  $v_{\perp}^O$  indicate this velocity is extremely small, in fact no growth in this direction was observed. Thus to the accuracy of the current work  $v_{\perp}^O \approx 0$ . The reason for this slow growth is that the modulated solution is very similar to the amplitude of the ordered solution and consequently the spatial transition from the ordered to modulated phase can be extremely sharp. In the limit of an infinitely sharp interface  $\sigma \rightarrow \infty$  and  $v \rightarrow 0$ .

The results of these calculations indicate that for quenches from the disordered phase the droplets will grow asymmetrically in a direction perpendicular to the lamella, leading to elongated lamella structures since  $v_{\parallel}^D < v_{\perp}^D$ . In contrast, for quenches from the ordered phase  $v_{\parallel}^D > v_{\perp}^D$ . Thus a small spherical nucleated droplet will tend to sprout arms which will invade the neighboring territory. This growth leads to a labyrinth type struc-

ture similar to that observed in reacting chemical fronts [8].

To illustrate the remarks of the preceding paragraphs several numerical simulations were conducted, which are illustrated in Fig. (3). The numerical algorithm is discussed in a previous paper [4] and is based on the cell dynamics method [9]. Figures (3a) and (3b) respectively show transient patterns that emerge from quenches from the disordered regime to just below and far below  $T_{OM}$ . The highly interconnected morphology shown in Fig. (3a) is a long-lived metastable modulated structure that typically evolves only near defects. The deeper quench (Fig. (3b)) shows that regions of high interface curvature coincide with large concentrations of terminal droplets, thus indicating the droplets inhibit interface relaxation and domain growth. Figures (3c) and (3d) are transient patterns obtained by the nucleation of the modulated phase from quenches from the disordered and ordered regimes respectively. These figures show the lamellar and labyrinthine type structures predicted in the preceding paragraphs.

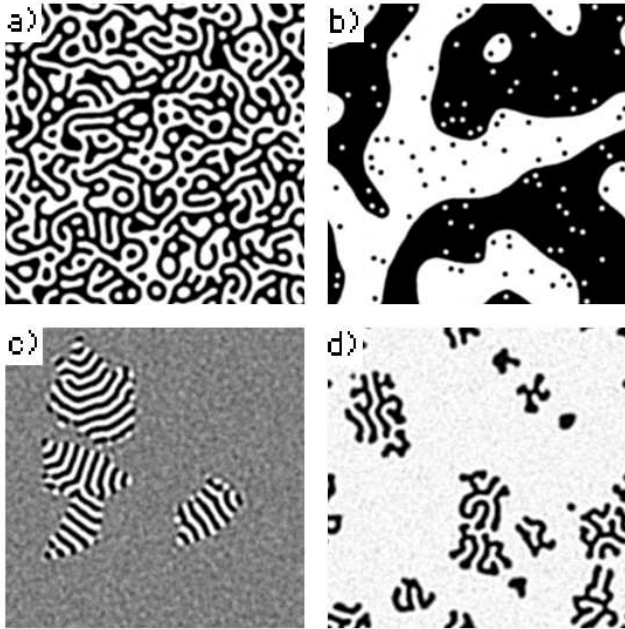


FIG. 3. Figures (a) and (b) are the transient patterns that emerge following quenches from a disordered state. Figures (a) and (b) are at  $\tau = 182$  and  $\tau = 329$  at quench temperatures of  $T = T_{OM} - 4K$  and  $T = T_{OM} - 44K$  respectively. Figure (c) is a pattern obtained by quenching from the disordered state into the modulated regime at  $T = T_{OM} + 39.5K$  at  $\tau = 57.3$ . Figure (d) is a pattern obtained by quenching from the ordered state into the modulated regime at  $T = T_{OM} + 38K$  at  $\tau = 84.0$ .

In summary several predictions for the kinetics of phase transformations in CuAu have been made. For quenches from the disordered to just below the ordered/modulated transition it is predicted that linear

dispersion will produce a modulated morphology. This modulated structure will be long-lived since the modulated phase is metastable in the ordered regime. For quenches far below  $T_{OM}$  it was found that the formation of the ordered phases are strongly inhibited by the appearance of terminal drops. Growth in this region will be much slower than standard order/disorder transitions since the droplets collect at antiphase boundaries and inhibit motion. For quenches into the modulated phases it was found the initial state played an important role in determining the transient morphologies. Quenches from the ordered and disordered region respectively produced labyrinthine and lamellar type structures.

Finally it is interesting to speculate on the asymptotic dynamics in the modulated regime. In this case the dynamics are controlled by the elimination of defects and the relaxation of the orientation of the individual lamella. Similar dynamics occur in the Swift Hohenberg [10] model of Rayleigh-Bénard convection and lead to the growth of domains of the same orientation growing at rate of  $t^{1/4}$  in the presence of thermal fluctuations and  $t^{1/5}$  in the absence of fluctuations [11]. It is likely the same growth exponent would be measured in this system.

The authors would like to thank Bill Klein, Oana Malis and Karl Ludwig for many useful discussions. KRE acknowledges support of grant NSF-DMR-8920538 administered through the U. of Illinois Materials Research Laboratory. The work of BC and NAG was supported by NSF grants DMR-9208084 (BC) and DMR-952093 (NAG). NG acknowledges support from NSF through grant DMR-93-14938.

- 
- [1] B. Chakraborty and Z. Xi, Phys. Rev. Lett **68**, 2039 (1992).
  - [2] K. W. Jacobsen, J. K. Norskov and M. J. Puska, Phys. Rev. B **35**, 7423 (1987)
  - [3] K. W. Jacobsen, Comments Cond. Mat. Phys. **14**, 129 (1988).
  - [4] B. Chakraborty, K. Elder and N. Goldenfeld, Physica **A224**, 113 (1996).
  - [5] B. Chakraborty, Phys. Rev. B **49**, 8608 (1994).
  - [6] S. Allen and J. Cahn, Acta Metall. **23**,1 (1975).
  - [7] J. D. Gunton, M. San Miguel and P. Sahni, in *Phase Transitions and Critical Phenomena*, edited by C. Domb and J. L. Lebowitz
  - [8] D. M. Petrich and R. E. Goldstein, Phys. Rev. Lett. **72**, 1120 (1994).
  - [9] Y. Oono and S. Puri, Phys. Rev. A **58**, 836 (1987).
  - [10] J. Swift and P. C. Hohenberg, Phys. Rev. A **15**, 319 (1977).
  - [11] K. R. Elder, J. Viñals and M. Grant, Phys. Rev. A **46**, 7618 (1993); Phys. Rev. Lett. **68**, 3024 (1992).